Volume 1 | Number 1 | Jan 2013 | Pages 1–100

ChemComm

Chemical Communications
www.rsc.org/chemcomm

ROYAL SOCIETY OF CHEMISTRY

ROYAL SOCIETY OF CHEMISTRY

www.rsc.org/chemcomm

ChemComm

COMMUNICATION

Metal-free hydrogen evolution with nanoparticles derived from pyrene via two-photon ionization induced by laser irradiation†

Kei Ohkubo,[*ab] Naoki Kohno,[a] Yusuke Yamada[ac] and Shunichi Fukuzumi[*abd]

Laser irradiation of a cyclohexane solution containing pyrene resulted in hydrogen evolution as pyrene was converted to a metal-free nanoparticle photocatalyst. When C_6H_{12} was replaced by C_6D_{12}, D_2 was mainly evolved. This result suggests that hydrogen source is cyclohexane used as a solvent. Photocatalytic hydrogen evolution was also observed in an aqueous solution by using a water-soluble pyrene derivative.

Various approaches to the light energy conversion into chemical energy have been developed in artificial photosynthesis.[1-4] Heterogeneous metallic nanoparticles composed of semiconductor metallic oxides have been widely used for water splitting as catalysts of hydrogen production from water.[5-8] However, the catalytic mechanism of hydrogen evolution has yet to be clarified. On the other hand, molecular metal-free photocatalysis under the homogeneous conditions has recently merited special attention in organic synthesis, physical chemistry and green chemistry because of its low cost and mild reaction conditions for activation of substrates.[9-13] Preparation of organic nanocrystals has been established by the laser induced decomposition of organic crystals and particles.[14-18] However, there have been few reports on photocatalytic reactions using heterogeneous organic nanoparticles as a metal-free photocatalyst.[19,20]

Pyrene is known as an organic photosensitizer in the photochemical reactions. Two-photon excitation of pyrene produces the photoionization products, pyrene radical cation and a solvated electron under the homogeneous conditions. The one-electron oxidation and reduction potential of pyrene is +1.3 and -2.0 V *vs.* SCE in MeCN.[21,22] Pyrene radical anion is generated by two-photon excitation and one-electron reduction by the solvated electron [e⁻(solv)] or photoinduced electron transfer between the excited state of a pyrene molecule (S2 or S1 state) and the ground state of another pyrene molecule due to the higher-lying excited state $(E(S1) = 3.34$ eV$)$[23-26] than the HOMO-LUMO gap

(3.30 eV) in polar solvent. In nonpolar solvent, the solvated electron may have strong reducing ability to reduce proton (H^+) to hydrogen (H_2) without metal catalyst.

H_2 is primarily used in the chemical industry as a reactant being proposed as an alternative energy source in future. Catalytic H_2 evolution systems have extensively been studied by using sacrificial electron donors, photosensitisers and electron mediators such as methyl viologen and an H_2 evolution catalyst such as platinum catalyst.[27-32] However, there has been no report on photocatalytic H_2 evolution systems via proton reduction using an organic photosensitiser alone without any sacrificial electron source.

We report herein that metal-free photoinduced H_2 evolution has been made possible by using pyrene as a precursor of nanoparticles. Efficient H_2 evolution was observed in various organic solvents as well as water using pyrene alone as a metal-free organic photocatalyst under laser light irradiation at room temperature under atmospheric pressure. The reaction mechanism of laser-induced H_2 evolution has been clarified based on the oxidized products, deuterium kinetic isotope effects and the dependence of the rate of H_2 evolution on the laser intensity.

Nanosecond laser flash irradiation ($\lambda = 355$ nm, 10 Hz, 40 mJ pulse⁻¹, i.d. 8 mm) of a deaerated cyclohexane solution containing pyrene (50 mM) for 90 min resulted in formation of highly dispersed black nanoparticles in the solution. Fig. 1 shows UV-vis absorption spectral change in the laser irradiation of pyrene in cyclohexane. The characteristic absorption bands at 306, 319 and 334 nm due to pyrene observed before irradiation disappeared and turned to the broad absorption from UV-vis-near-IR region.

To characterize the nanoparticles, dynamic light scattering (DLS) measurements were performed for the photochemically growing nanoparticles. The nanoparticles of 420 nm in size were observed after laser irradiation for 30 min as shown in Fig. 2a.
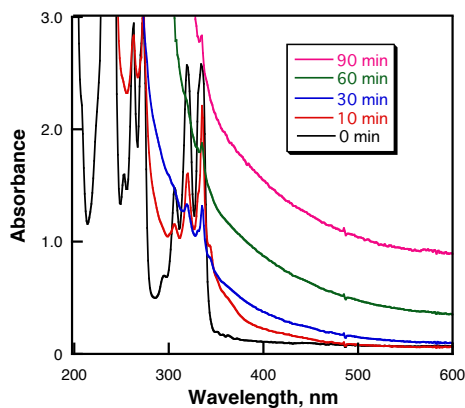
Fig. 1 UV-vis absorption spectral changes for growing pyrene nanoparticles observed in a cyclohexane solution (2.5 mL) containing pyrene (50 mM) under laser irradiation (λ = 355 nm; 40 mJ pulse^{-1}; 10 pulse s^{-1}).
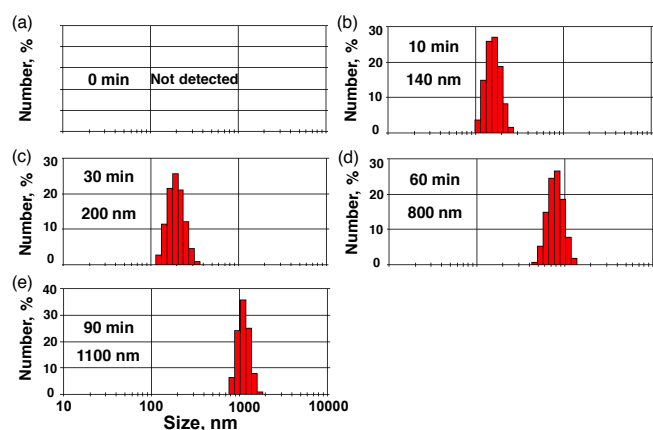

Fig. 2 Time course of DLS data of a cyclohexane solution (2.5 mL) containing pyrene (50 μM) under laser irradiation (λ = 355 nm; 40 mJ pulse^{-1}; 10 Hz).
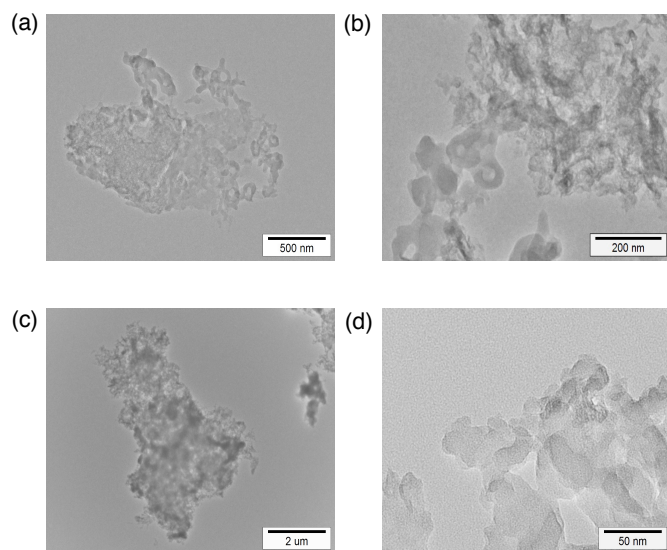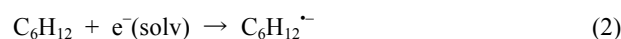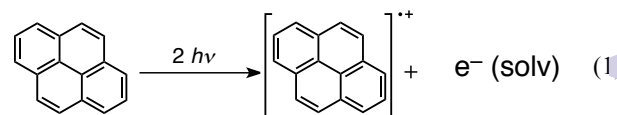

Fig. 3 TEM images of (a) a cyclohexane solution (2.5 mL) of pyrene (50 μM) after laser light irradiation (λ = 355 nm; 40 mJ pulse^{-1}; 10 pulse s^{-1}) for 30 min, (b) magnified figure of (a), (c) dispersion liquid of precipitation after laser light irradiation (λ = 355 nm; 40 mJ pulse^{-1}; 10 pulse s^{-1}) for 90 min and (d) magnified figure of (c).

The particle size grows by further laser irradiation to afford nanoparticles of 1100 nm in size after 90 min irradiation. Transmission electron microscopy (TEM) measurements were performed to evaluate the transformation of pyrene nanoparticles after laser irradiation. TEM images after photoirradiation for 30 min (Fig. 3a and b) clearly exhibit small nanoparticles. After irradiation for 90 min, the size of nanoparticles was enlarged (Fig. 3c and d). The IR spectra of nanoparticles showed that the characteristic peak at 3043 cm^{-1} due to the C–H vibration disappeared and it was blue-shifted to 2925 cm^{-1} with an increase in irradiation time (see Fig. S1 in the electronic supplementary information (ESI)†). This suggests that C-H bonds of pyrene were broken in growing nanoparticles. To obtain the information of C-H bond of pyrene in the nanoparticle, CHN elemental analysis was performed in growing nanoparticles. The ratio of carbon and hydrogen was 94.4 : 5.6, which is virtually the same as the comparison of pyrene alone (95.0 : 5.0). Thus, the main component in nanoparticle is the undamaged pyrene. The pyrene molecules on the particle surface may be dehydrogenated to form pyrene polymer by the C-C bond coupling reaction. The formation of pyrene oligomers was confirmed by the powder X-ray diffraction (PXRD) measurements (Fig. S2 in ESI†). The XRD patterns with peaks at 2θ = 11 and 24° due to the (0 0 1) and (2 2 0) planes was maintained after laser irradiation, indicating that the pyrene was not damaged in the nanoparticles.

Laser induced nanoparticle formation was initiated by the photo-ionization of pyrene to form pyrene radical cation and solvated electron [eqn (1)]. Hydrogen atom transfer from cyclohexane radical anion (Cy$^{\bullet-}$), which is produced by the reduction of cyclohexane by solvated electron [eqn (2)], to pyrene radical cation (Py$^{\bullet+}$) occurs to produce hydrogenated pyrene neutral radical (PyH$^{\bullet}$) and cyclohexyl radical (C$_6$H$_{11}$$^{\bullet}$) [eqn (3)]. Two molecules of PyH$^{\bullet}$ react to give the pyrene dimer and H$_2$ [eqn (4)]. The dimer was detected by MALDI-TOF-MS

$$\text{(pyrene)} \xrightarrow{2\,h\nu} \left[\text{(pyrene)} \right]^{\bullet+} + e^- \text{(solv)} \quad (1)$$

$$C_6H_{12} + e^-(\text{solv}) \rightarrow C_6H_{12}{}^{\bullet-} \quad (2)$$

$$Py^{\bullet+} + C_6H_{12}{}^{\bullet-} \rightarrow PyH^{\bullet} + C_6H_{11}{}^{\bullet} \quad (3)$$

$$2PyH^{\bullet} \rightarrow Py\text{-}Py + H_2 \quad (4)$$

measurements (see Fig. S3 in ESI†). The resulting C$_6$H$_{11}$$^{\bullet}$ is converted to cyclohexene by disproportionation, which was detected by GC-MS analysis (Fig. S4 in ESI†). Butadiene and propene were also detected as side products. The further oligomerization of pyrene occurred by laser irradiation to form the pyrene nano-aggregates.

On the basis of above mentioned reaction mechanism in eqn (4), the laser-induced dimerization of pyrene radicals results in H$_2$ evolution. H$_2$ evolution was successfully detected by GC experiments in the reaction of pyrene in cyclohexane under nanosecond laser irradiation at 355 nm as shown in Fig. 4. The
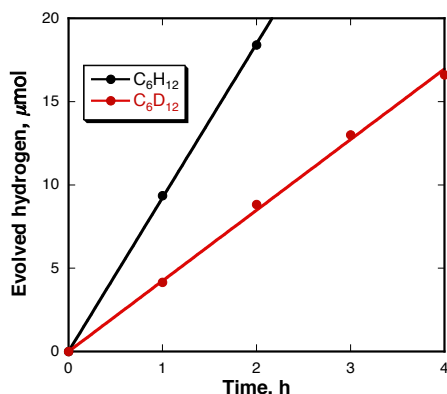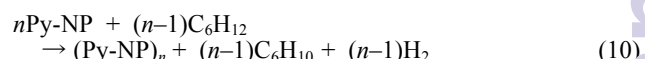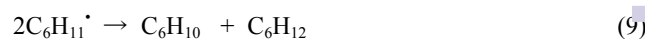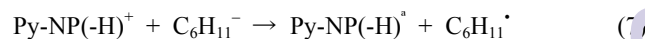
Fig. 4 Time courses of the amount of evolved H_2 and D_2 under laser irradiation (λ = 355 nm; 20 mJ pulse^{-1}; 10 pulse s^{-1}) of a cyclohexane or cyclohexane-d_{12} solution (2.5 mL) containing pyrene (0.5 mM).

TON of the catalysts for H_2 evolution was 2,000 for 7 h based on the initial moles of pyrene in cyclohexane where the reaction conditions are [Py] = 50 μM, 40 mJ/pulse at λ = 355 nm in cyclohexane (2.5 mL). No deactivation was observed in laser irradiation for 7 h (Fig. S5 in ESI†). When cyclohexane was replaced by cyclohexane-d_{12} as a solvent, D_2 gas was selectively evolved (data are shown in Fig. S6 in ESI†).[33] The kinetic isotope effect (KIE) value for the H_2 evolution was determined to be 2.1. Thus, the rate-determining step of H_2 evolution is carbon-hydrogen bond cleavage of cyclohexane radical anion in hydrogen atom transfer to pyrene radical cation. Indeed, no H_2 evolution was observed in cyclohexene instead of cyclohexane (Fig. S7 in ESI†). H_2 evolution also occurred when laser light excitation wavelength was changed from 355 nm to 532 nm by Nd:YAG laser as a light source (Fig. S8 in ESI†) because pyrene nanoparticles show strong and broad absorption band covering whole visible region as previously shown in Fig. 1.

The dependence of the rate of H_2 evolution on the laser intensity was examined using different laser power intensities at 355 nm (0–20 mJ pulse^{-1}) as shown in Fig. 5a. The initial rates of H_2 evolution are proportional to the second power of the laser intensity as shown in Fig. 5b. This suggests that an ionization reaction of two-photon absorbed species may be involved in the photocatalytic H_2 evolution. The maximum quantum yield observed was 7.9% when the laser power is 40 mJ per pulse at 355 nm. The efficiency of the photocatalytic H_2 evolution is affected by the solvent polarities as shown in Table 1. The efficiency of photocatalytic H_2 evolution is highest for cyclohexane and lowest for dimethylsulfoxide in the series of solvents.[34] This suggests that electron reducing ability of solvated electron generated by photoionizaton of pyrene in non-polar cyclohexane is much higher than in the polar solvent due to the stabilization of solvated electron.

On the basis of the above-mentioned results, the reaction mechanism of photocatalytic H_2 evolution from pyrene nanoparticles (Py-NP) in cyclohexane (CyH) is shown in eqns (5)-(9). Two-photon ionization of Py-NP is much easier than pyrene monomer, yielding Py-NP radical cation (Py-NP$^{\bullet+}$) and cyclohexane radical anion ($C_6H_{12}{}^{\bullet-}$) [eqn (5)]. Hydrogen atom transfer from $C_6H_{12}{}^{\bullet-}$ to Py-NP$^{\bullet+}$ occurs [eqn (6)], followed by electron transfer from $C_6H_{11}{}^-$ to Py-NP(-H)$^+$ [eqn (7)] and radical coupling with release of H_2 [eqn (8)]. Cyclohexyl radical ($C_6H_{11}{}^\bullet$) disproportionate to yield cyclohexene and cyclohexane [eqn (9)]. The total stoichiometry is given by eqn (10) by summing up eqns (5)-(9).

$$Py\text{-}NP + C_6H_{12} + 2\,h\nu \rightarrow Py\text{-}NP^{\bullet+} + C_6H_{12}{}^{\bullet-} \quad (5)$$

$$Py\text{-}NP^{\bullet+} + C_6H_{12}{}^{\bullet-} \rightarrow Py\text{-}NP(\text{-}H)^+ + C_6H_{11}{}^- \quad (6)$$

$$Py\text{-}NP(\text{-}H)^+ + C_6H_{11}{}^- \rightarrow Py\text{-}NP(\text{-}H)^a + C_6H_{11}{}^\bullet \quad (7)$$

$$2Py\text{-}NP(\text{-}H)^a \rightarrow (Py\text{-}NP)_2 + H_2 \quad (8)$$

$$2C_6H_{11}{}^\bullet \rightarrow C_6H_{10} + C_6H_{12} \quad (9)$$

$$nPy\text{-}NP + (n-1)C_6H_{12} \\ \rightarrow (Py\text{-}NP)_n + (n-1)C_6H_{10} + (n-1)H_2 \quad (10)$$
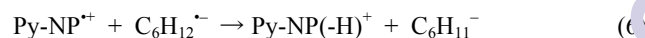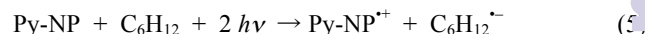
No nanoparticle of pyrene was formed in an aqueous solution by the laser photoirradiation at 355 nm. Thus, no H_2 evolution
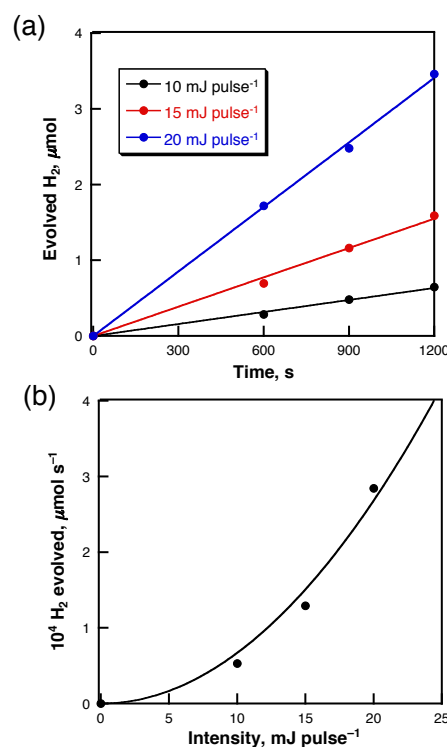

Fig. 5 (a) Time courses of the amount of evolved H_2 in cyclohexane (2.5 mL) containing pyrene particles (0.25 mg) under laser light irradiation (λ = 355 nm; 10, 15 or 20 mJ pulse^{-1}; 10 pulse s^{-1}) and (b) Plot of rate of H_2 evolution vs laser intensity. A fitted line was drawn by second-order function.

Table 1 Rates of evolved H_2 from Py-NP in various solvents.[a]

Solvent	Dielectric constant	H_2, μmol h^{-1}
n-Heptane	1.9	5.7
Cyclohexane	2.0	14
2-Propanol	18	2.6
Acetone	20	3.2
Acetonitrile	37	4.6
Dimethylsulfoxide	47	0.1

[a] Conditions: solvent: 2.5 mL; pyrene: 0.50 mM; nanosecond laser (λ = 355 nm; 20 mJ pulse^{-1}; 10 pulse s^{-1}), under N_2.

was observed under photoirradiation. When pyrene was replaced by sodium pyrene-1-acetate used as a water-soluble photosensitiser, the nanoparticle formation and H_2 evolution occurred in an aqueous solution under otherwise the same reaction conditions (Fig. S9 in ESI†). We also examined H_2 evolution using other hydrocarbons instead of pyrene. Nanoparticles were also formed under the same laser-irradiation conditions. Nanoparticles of coronene and 9,10-diphenylanthracene were effective as an H_2-evolution photocatalyst. However, the rates of H_2 evolution were 1.4, 1.1 and 0 μmol h^{-1} for 9,10-diphenylanthracene, coronene and rubrene, respectively, which are significantly slower than the value of pyrene (4.6 μmol h^{-1}) in acetonitrile. In the case of rubrene as a red dye, no nanoparticle was formed without H_2 evolution. It is difficult to form the oligomers as a precursor of H_2-evolution catalyst because of the more delocalized π-radical cation than pyrene radical cation. In particular, the radical cations of rubrene and 9,10-diphenyl-anthracene are very stable in solution without any reaction such as dimerization.

In conclusion, pyrene nanoparticles have been demonstrated to act as efficient metal free organic photocatalysts for H_2 evolution from various solvents. Cyclohexane used as a solvent is the most effective hydrogen source in H_2 evolution with pyrene nanoparticles. The rate of H_2 evolution increased with increasing the laser intensity, exhibiting a second power dependence, because H_2 was evolved via the two-photon ionization of pyrene followed by hydrogen atom transfer from cyclohexane radical anion to pyrene radical cation. Pyrene radical cations dimerise to form oligomer nanoparticles as a more effective photocatalyst for H_2 evolution. This is the first report of catalytic H_2 evolution using an organic nanoparticle photocatalyst without inorganic material.

Notes and references

^{a} Department of Material and Life Science, Graduate School of Engineering, Osaka University, ALCA and SENTAN, Japan Science and Technology Agency (JST), Suita, Osaka 565-0871, Japan.

^{b} Department of Bioinspired Science, Ewha Womans University, Seoul 120-750, Korea

^{c} Department of Applied Chemistry & Bioengineering, Graduate School of Engineering, Osaka City University, 3-3-138 Sugimoto, Sumiyoshi-ku, Osaka 558-8585, Japan

^{d} Faculty of Science and Technology, Meijo University and ALCA and SENTAN, Japan Science and Technology Agency (JST), Tempaku, Nagoya, Aichi 468-8502, Japan

† Electronic Supplementary Information (ESI) available: Experimental and spectroscopic details. See DOI: 10.1039/c4cc00000x/

1   J. Barber, *Chem. Soc. Rev.*, 2009, **38**, 185-196.
2   N. S. Lewis and D. G. Nocera, *Proc. Natl. Acad. Sci. U. S. A.* 2006, **103**, 15729-15735.
3   R. E. Blankenship, D. M. Tiede, J. Barber, G. W. Brudvig, G. Fleming, M. Ghirardi, M. R. Gunner, W. Junge, D. M. Kramer, A. Melis, T. A. Moore, C. C. Moser, D. G. Nocera, A. J. Nozik, D. R. Ort, W. W. Parson, R. C. Prince and R. T. Sayre, *Science*, 2011, **332**, 805-809.
4   M. G. Walter, E. L. Warren, J. R. McKone, S. W. Boettcher, Q. X. Mi, E. A. Santori and N. S. Lewis, *Chem. Rev.*, 2010, **110**, 6446-6473.
5   M. Hambourger, A. Brune, D. Gust, A. L. Moore and T. A. Moore, *Photochem. Photobiol.*, 2005, **81**, 1015-1020.
6   R. Abe, K. Hara, K. Sayama, K. Domen and H. Arakawa, *J. Photochem. Photobiol. A*, 2000, **137**, 63-69.
7   E. Reisner, D. J. Powell, C. Cavazza, J. C. Fontecilla-Camps and F. A. Armstrong , *J. Am. Chem. Soc.*, 2009, **131**, 18457-18466.
8   A. Le Goff, V. Artero, B. Jousselme, P. D. Tran, N. Guillet, R. Métayé, A. Fihri, S. Palacin and M. Fontecave, *Science*, 2009, **326**, 1384-1387.
9   (*a*) P. D. Morse and D. A. Nicewicz, *Chem. Sci.*, 2015, **6**, 270-274; (*b*) J. Gesmundo and Nicewicz, D. A. *Beilstein J. Org. Chem.*, 2014, **10**, 1272-1281.
10 C. K. Prier, D. A. Rankic and D. W. C. MacMillan, *Chem. Rev.*, 2013, **113**, 5322–5363.
11 A. Aguirre-Soto, C-.H. Lim, A. T. Hwang, C. B. Musgrave and J. W. Stansbury, *J. Am. Chem. Soc.*, 2014, **136**, 7418-7427.
12 (*a*) S. Fukuzumi, K. Ohkubo and T. Suenobu, *Acc. Chem. Res.*, 2014, **47**, 1455-1464; (*b*) S. Fukuzumi and K. Ohkubo, *Chem. Sci.*, 2013, **4**, 561-574; (*c*) S. Fukuzumi and K. Ohkubo, *Org. Biomol. Chem.*, 2014, **12**, 6059-6071.
13 E. Bernoud, C. Lepori, M. Mellah, E. Schulz and J. Hannedouche, *Catal. Sci. Technol.*, 2015, **5**, 2017-2037
14 (*a*) T. Asahi, T. Sugiyama and H. Masuhara, *Acc. Chem. Res.*, 2008, **41**, 1790-1798; (*b*) T. Sugiyama, S.-i. Ryo, I. Oh, T. Asahi and H. Masuhara, *J. Photochem. Photobiol. A Chem.*, 2009, **207**, 7-12.
15 H. Tabata, M. Akamatsu, M. Fujii and S. Hayashi, *Jpn. J. Appl. Phys.*, 2007, **46**, 4338-4343.
16 A. Ibanez, S. Maximov, A. Guiu, C. Chaillout and P. L. Baldeck. *Adv. Mater.*, 1998, **10**, 1540-1543.
17 J. Ye, H.-Z. Chen and M. Wang, *J. Mater. Sci.*, 2003, **38**, 4021-4025.
18 A. H. Matsui, K. Mizuno, O. Nishi, Y. Matsushima, M. Shimizu, T. Goto and M. Takeshima, *Chem. Phys.*, 1995, **194**, 167-174.
19 (*a*) X. Wang, K. Maeda, A. Thomas, K. Takanabe, G. Xin, J. M. Carlsson, K. Domen and M. Antonietti, *Nature Mater.*, 2009, **8**, 76-80; (*b*) Y. Cui, Z. Ding, X. Fu and X. Wang, *Angew. Chem., Int. Ed.*, 2012, **51**, 11814-11818; (*c*) Z. Lin and X. Wang, *Angew. Chem., Int. Ed.*, 2013, **52**, 1735-1738; (*d*) Y. Zheng, L. Lin, X. Ye, F. Guo and X. Wang, *Angew. Chem., Int. Ed.*, 2014, **53**, 11926-11930; (*e*) G. Zhang, M. Zhang, X. Ye, X. Qin, S. Lin and X. Wang, *Adv. Mater.*, 2014, **26**, 805-809.
20 K. Ohkubo, N. Kohno, Y. Yamada and S. Fukuzumi, *Chem. Sci.*, 2015, **6**, 666-674.
21 S. Fukuzumi, K. Ohkubo, H. Imahori and D. M. Guldi, *Chem.–Eur. J.*, 2003, **9**, 1585-1593.
22 S. Fukuzumi, J. Yuasa, N. Satoh and T. Suenobu, *J. Am. Chem. Soc.*, 2004, **126**, 7585-7594.
23 J. T. Richards, G. West and K. T. John, *J. Phys. Chem.*, 1970, **74**, 4137.
24 A. R. Watkins, *J. Phys. Chem.*, 1976, **80**, 713-717.
25 X. Chen, S. Shen, L. Guo and S. S. Mao, *Chem. Rev.*, 2010, **110**, 6503.
26 M. G. Walter, E. L. Warren, J. R. McKone, S. W. Boettcher, Q. E. A. M. Santori and N. S. Lewis, *Chem. Rev.*, 2010, **110**, 6446-6470.
27 W. J. Youngblood, S.-H. A. Lee, K. Maeda and T. E. Mallouk, *Acc. Chem. Res.*, 2009, **42**, 1966-1972.
28 A. Kudo and Y. Miseki, *Chem. Soc. Rev.*, 2009, **38**, 253-278.
29 R. M. Navarro, M. C. A. Galván, J. A. V. de la Mano, S. M. Al-Zahrani and J. L. G. Fierro, *Energy Environ. Sci.*, 2010, **3**, 1865-1882.
30 H. Zhou, T. Fan and D. Zhang, *ChemSusChem*, 2011, **3**, 513-528.
31 (*a*) K. Maeda, K. Teramura, D. Lu, T. Takata, N. Saito, Y. Inoue and K. Domen, *Nature*, 2006, **440**, 295; (*b*) K. Maeda, M. Higashi, D. Lu, R. Abe and K. Domen, *J. Am. Chem. Soc.*, 2010, **132**, 5858-5868.
32 (*a*) H. Kotani, K. Ohkubo, Y. Takai and S. Fukuzumi, *J. Phys. Chem. B*, 2006, **110**, 24047-24053; (*b*) H. Kotani, T. Ono, K. Ohkubo and S. Fukuzumi, *Phys. Chem. Chem. Phys.*, 2007, **9**, 1487-1492; (*c*) H. Kotani, R. Hanazaki, K. Ohkubo, Y. Yamada and S. Fukuzumi, *Chem.-Eur. J.*, 2011, **17**, 2777-2785.
33 HD was formed by the detection with GC as shown in Fig. S6a in ESI. HD is a coupling product in the reaction of PyD˙ and PyH˙ [(eqn. (4)].
34 Lower H_2 formation efficiency in more non-polar *n*-heptane than cyclohexane may result from the lower numbers of weak secondary C–H bonds in *n*-heptane.

Graphical abstract image
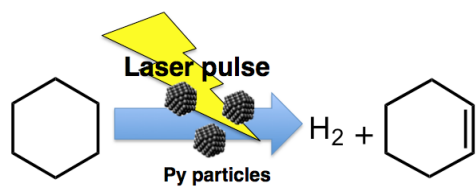
H_2 evolution occurred efficiently with nanoparticles of pyrene oligomers produced by the two-photon laser excitation in cyclohexane.